iScience

CellPress
OPEN ACCESS

Article

OVOL2 induces autophagy-mediated epithelial-mesenchymal transition by the ERK1/2 MAPK signaling in lung adenocarcinoma

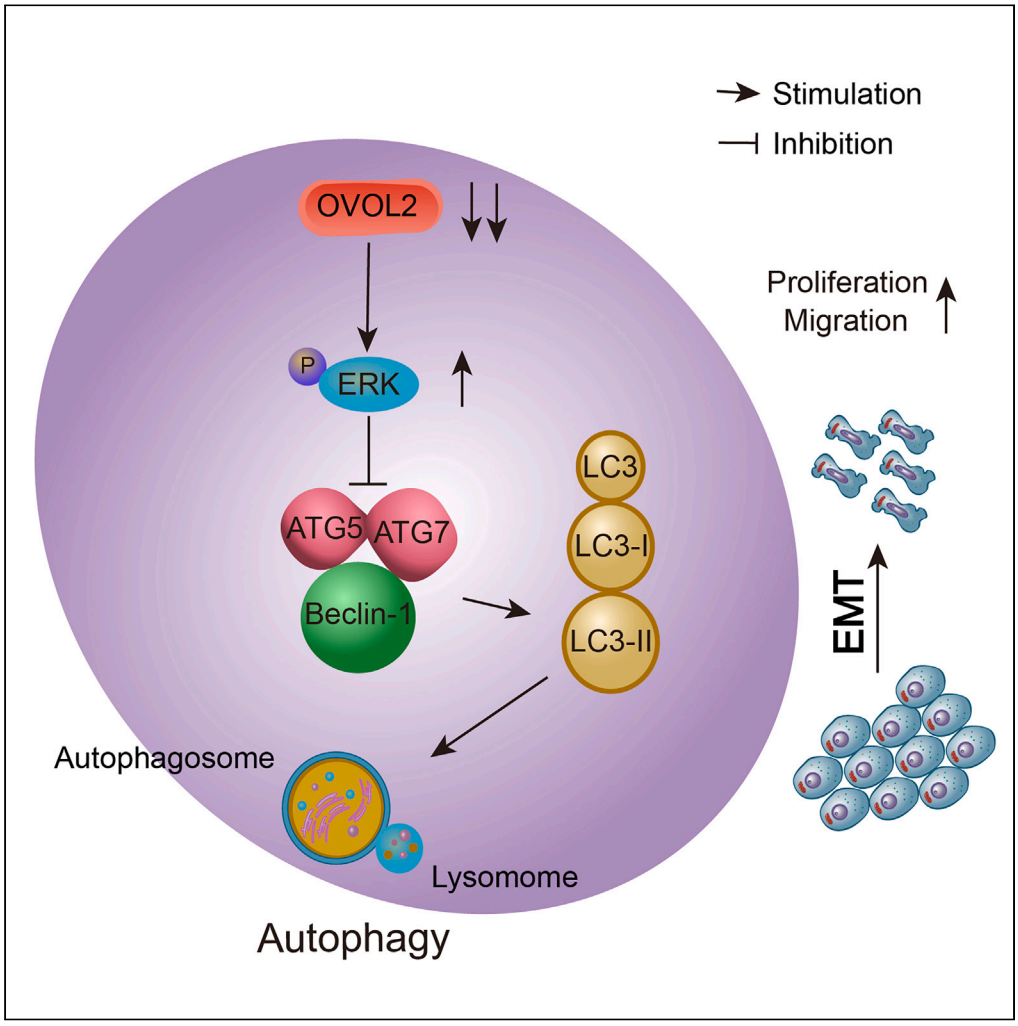

Yali Wang, Lin Shi, Yuchao He, ..., Zhiyong Liu, Peng Chen, Hua Guo

liuzhiyong@tjmuch.com (Z.L.)
chenpengdoc@sina.com (P.C.)
guohua@tjmuch.com (H.G.)

Highlights

OVOL2 can function as a specific biomarker in LUAD

OVOL2 inhibits EMT and malignant biological behaviors in LUAD

Autophagy is a key step in regulating the expression of OVOL2 and inducing EMT in LUAD

OVOL2 regulates autophagy through the MAPK signaling pathway in LUAD

Wang et al., iScience 27, 108873
February 16, 2024
https://doi.org/10.1016/j.isci.2024.108873

iScience

CellPress
OPEN ACCESS

Article

OVOL2 induces autophagy-mediated epithelial-mesenchymal transition by the ERK1/2 MAPK signaling in lung adenocarcinoma

Yali Wang,[1,2,3,5,7] Lin Shi,[1,2,3,6,7] Yuchao He,[1,3,7] Wenchen Gong,[3,4] Yanyan Cui,[5] Ran Zuo,[1,2,3] Yu Wang,[1,2,3] Yi Luo,[1,3] Liwei Chen,[1,3] Zhiyong Liu,[1,3,*] Peng Chen,[2,3,*] and Hua Guo[1,3,8,*]

SUMMARY

Lung adenocarcinoma (LUAD) is one of the leading causes of cancer-related death worldwide. Epithelial-mesenchymal transition (EMT) plays an important role in malignant tumor progression. Recently, accumulating evidence has shown that autophagy is involved in the regulation of EMT-induced migration. Therefore, the exploration of targets to inhibit EMT by targeting autophagy is important. In this study, we found that OVO-like zinc finger 2 (OVOL2) may be a key target for regulating autophagy-induced EMT. Firstly, we found that OVOL2 expression was dramatically downregulated in LUAD. Low expression of OVOL2 is an indicator of poor prognosis in LUAD. *In vitro* experiments have shown that downregulation of OVOL2 expression induces EMT, thereby promoting malignant biological behavior, such as proliferation, migration, and invasion of LUAD cells. Interestingly, autophagy is a key step in regulating OVOL2 and inducing EMT. Furthermore, OVOL2 regulates autophagy through the MAPK signaling pathway, ultimately inhibiting the malignant progression of LUAD.

INTRODUCTION

Lung cancer is the second most common malignancy and the leading cause of death worldwide.[1,2] An estimated 2 million new cases and 1.76 million deaths are reported each year.[3] Lung adenocarcinoma (LUAD) has become the most common lung cancer subtype, accounting for more than 50% of cases, and its incidence is increasing.[4] However, the prognosis for patients is often poor, as most patients have advanced disease at the time of diagnosis, with a 5-year survival rate of less than 20%.[5]

Tumor metastasis is the leading cause of cancer-related mortality.[6] Metastasis is a complex biological process that is difficult to treat.[7] Epithelial mesenchymal transition (EMT) is key to the metastatic process and is considered an essential step by which epithelial-derived malignant tumor cells acquire the ability to migrate and invade. Among the biological processes, autophagy, which is a self-degrading process, has recently been reported to be instrumental in cancer cell metastasis.[8] Increasing evidence demonstrates that these two processes are intricately intertwined in metastasis. Autophagy plays an important role in the regulation of EMT. For example, in melanoma, Atg3, Atg5, Atg9, and Atg12 knockout-induced autophagy deficiency, increased p62 levels, decreased E-cadherin expression and promoted cell migration, invasion, and proliferation.[9] In human osteosarcoma cells, autophagy promotes invasion and metastasis by activating the EMT.[10] More importantly, targeting the interaction between EMT and autophagy has potential for cancer prevention and therapy.[11] Therefore, blocking EMT and autophagy is theoretically a promising anti-tumor strategy. However, reports on the specific regulatory relationship between them are few and thus deserve further investigation.

OVOL2, a member of the OVO family of conserved zinc-finger transcription factors, is thought to have originally regulated embryonic development and sperm formation.[12,13] In recent years, research has shown that OVOL2 plays an important role in the initiation and development of many tumors. The main function of OVOL2 is to inhibit cell proliferation, promote cell differentiation, and maintain the epithelial differentiation state.[14] A study in colorectal cancer showed that OVOL2 attenuates the expression of MAP3K8 to suppress EMT,[15] and a study in cutaneous squamous cell carcinoma showed that OVOL2-mediated ZEB1 downregulation can prevent the promotion of actinic keratosis.[16] A study on osteosarcoma showed that OVOL2 induces EMT by targeting ZEB1.[17] However, the role and mechanism of OVOL2 in tumors must be further investigated.

[1]Department of Tumor Cell Biology, Tianjin Medical University Cancer Institute and Hospital, Tianjin 300060, China
[2]Department of Thoracic Oncology, Lung Cancer Diagnosis and Treatment Center, Tianjin Medical University Cancer Institute and Hospital, Tianjin 300060, China
[3]National Clinical Research Center for Cancer, Key Laboratory of Cancer Prevention and Therapy, Tianjin's Clinical Research Center for Cancer, National Key Laboratory of Druggability Evaluation and Systematic Translational Medicine, Tianjin 300060, China
[4]Department of Pathology, Tianjin Medical University Cancer Institute and Hospital, Tianjin 300060, China
[5]Department of Oncology, Affiliated Hospital of Chifeng University, Chifeng, Inner Mongolia 024000, China
[6]Department of Oncology, Inner Mongolia Autonomous Region People's Hospital, Hohhot, Inner Mongolia 010000, China
[7]These authors contributed equally
[8]Lead contact
*Correspondence: liuzhiyong@tjmuch.com (Z.L.), chenpengdoc@sina.com (P.C.), guohua@tjmuch.com (H.G.)
https://doi.org/10.1016/j.isci.2024.108873

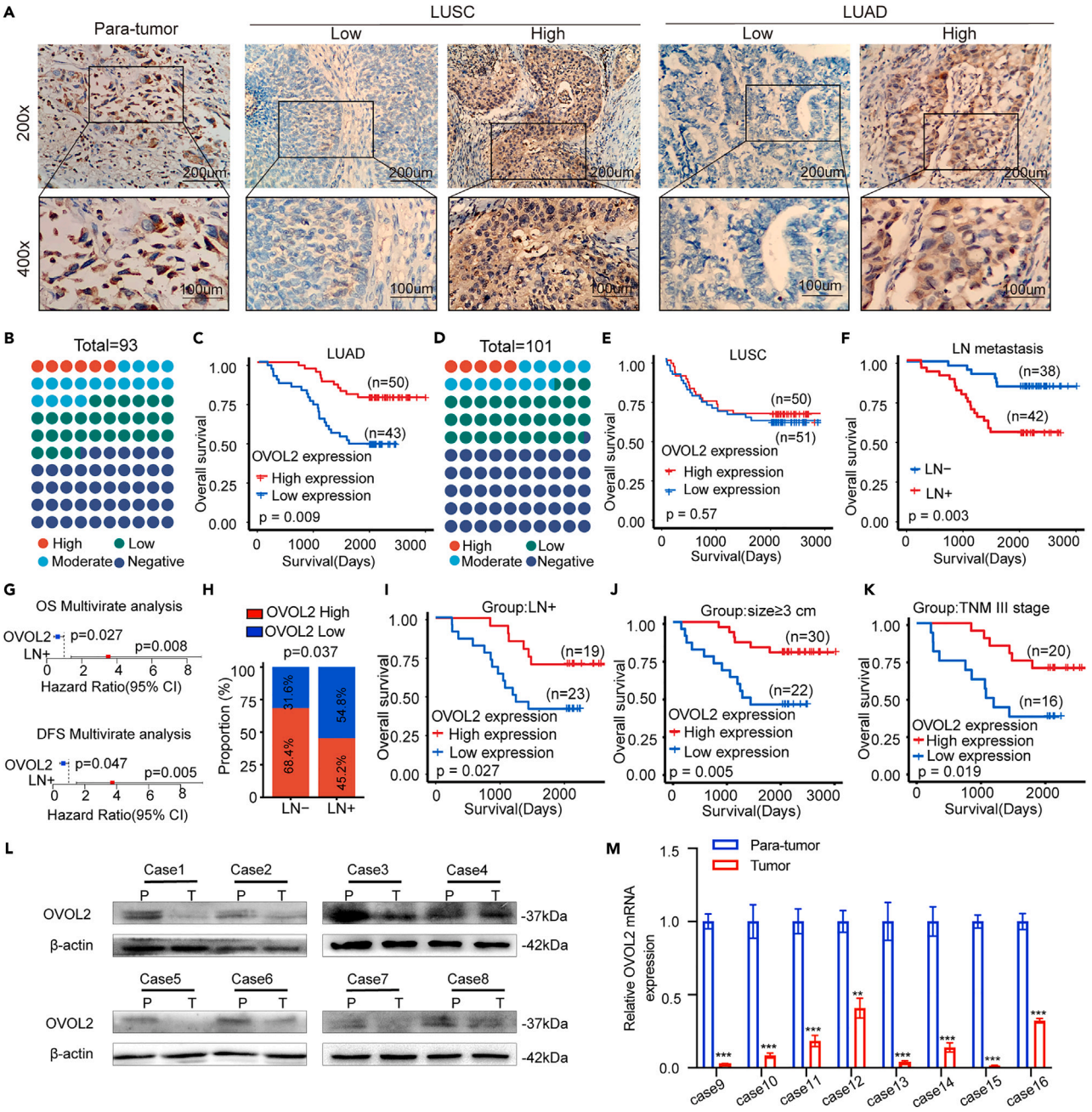

Figure 1. OVOL2 is a specific prognostic biomarker in LUAD

(A) IHC staining analysis of OVOL2 expression in tissue microarrays of lung cancer specimens.

(B) The proportions of LUAD patients with different OVOL2 expression levels.

(C) Kaplan-Meier survival curve showing the correlation between the OVOL2 IHC score and OS of LUAD patients.

(D) The proportions of LUSC patients with different OVOL2 expression levels.

(E) Kaplan-Meier survival curve analysis showing the correlation between the OVOL2 IHC score and OS in LUSC patients.

(F) Kaplan-Meier survival curve analysis showing the correlations between LN metastasis and OS in LUAD patients.

(G) Forest plots showing the multivariate risk factors of LUAD patients.

(H) Correlation analysis between the OVOL2 IHC score and LN metastasis.

(I) Kaplan-Meier survival curve showing the correlation between the OVOL2 IHC score and OS in a subgroup of LUAD patients (LN metastasis).

(J) Kaplan-Meier survival curve showing the correlation between the OVOL2 IHC score and OS in a subgroup of LUAD patients (tumor size ≥3cm).

Figure 1. *Continued*

(K) Kaplan-Meier survival curve showing the correlation between the OVOL2 IHC score and OS in a subgroup of LUAD patients (TNM stage III).

(L) Western blotting shows the differences in the OVOL2 protein between eight pairs of LUAD tissue and adjacent nonmalignant tissue.

(M) Real-time PCR showing the differences in the OVOL2 mRNA levels between eight pairs of LUAD tissue and adjacent nonmalignant tissue. *$p < 0.05$, **$p < 0.01$, ***$p < 0.001$. Data were expressed as the mean ± SDs.

In the current study, we demonstrated that OVOL2 was dramatically downregulated in LUAD tumor tissues, and low OVOL2 expression in patients with LUAD is indicative of poor prognosis. OVOL2 may serve as a specific prognostic biomarker of LUAD. More importantly, we demonstrated that downregulated OVOL2 promoted the occurrence of EMT by inhibiting autophagy. Low expression of OVOL2 induces autophagy by activating the MAPK signaling pathway, leading to the malignant progression of LUAD. Our results revealed a novel function of OVOL2 in tumor cells and may serve as a new therapeutic strategy for targeting OVOL2 in LUAD.

RESULTS

OVOL2 expression pattern and its correlation with prognosis in human LUAD

To verify the expression pattern of OVOL2 in lung cancer, a large cohort of 194 nonsmall cell lung cancer (NSCLC) samples (including 93 cases of LUAD and 101 cases of LUSC) was evaluated by immunohistochemistry (IHC) staining (Figure 1A). The results of 93 LUAD patients show that 46.5% of LUAD patient samples were negative for OVOL2 staining (Figure 1B). Furthermore, decreased OVOL2 expression was associated with poor overall survival (OS) and disease-free survival (DFS) (Figures 1C and S1A). We also examined OVOL2 expression in 101 patients with LUSC using IHC. The results showed that 50% of patients with LUSC had negative OVOL2 staining (Figure 1D). No significant association was found between OVOL2 expression and OS in LUSC ($p = 0.57$, Figure 1E). The same results were confirmed with OVOL2 expression in DFS ($p = 0.48$, Figure S1B). These results suggested that a unique relationship exists between the expression of OVOL2 and the prognosis of patients with LUAD.

We then analyzed the correlation between OVOL2 expression and other clinical indicators of LUAD. However, no significant correlation was found between OVOL2 expression and routine clinicopathological characteristics, such as age and gender. The Cox regression model showed that decreased OVOL2 expression and lymph node (LN) metastasis were independent risk factors for OS and DFS in LUAD (Figures 1F, and S1C; Tables S1 and S2). The results of multivariate analysis for OS and DFS in patients with LUAD are presented in forest plots (Figure 1G). This series of results indicated that OVOL2 could be used as a specific biomarker in LUAD patients. After removing missing data, a total of 23 out of 42 (54.8%) cases with LN metastasis had low OVOL2 expression levels. By contrast, only 12 out of 38 (31.6%) cases without LN metastasis had low OVOL2 expression levels ($p = 0.037$, Figure 1H). We further investigated the differential prognosis between high and low OVOL2 expression levels in three high-risk recurrence subgroups: LN metastasis, tumor size $\geq$3 cm and TNM stage III disease. Surprisingly, the patients with low OVOL2 expression still had worse OS among the three subgroups (Figures 1I–1K). A similar trend was estimated for DFS in the three subgroups (Figures S1D–S1F). Next, we selected eight pairs of fresh LUAD tissue samples and adjacent tissue samples for WB (Western Blotting) and verified that OVOL2 expression was significantly lower in LUAD tissues than in para tumor tissues (Figure 1L and S2A). The real-time PCR results showed a similar trend in the other eight pairs of tissue specimens (Figure 1M and Table S3). Thus, our results clearly indicate that OVOL2 is expressed at low levels in LUAD tissues, and low OVOL2 expression levels correlate with a poor prognosis. We reasoned that decreased OVOL2 expression may play an important role in LUAD progression and recurrence.

Knockdown of OVOL2 promotes LUAD cell proliferation, migration, and invasion *in vitro*

Next, we investigated the biological functions of OVOL2 in the TCGA database; GO (Gene Ontology) function analysis indicated that OVOL2 expression was associated with cell proliferation and metastasis (Figure S3A and Table S4). Firstly, we used PC9 and A549 cells to establish stable knockdown and overexpression cell lines. At the same time, we constructed the control cells sh-Ctrl and Vector, respectively. The efficiency of OVOL2 deletion and overexpression were confirmed by WB and real-time PCR (Figures 2A and S2B–S2E). Then, we evaluated the proliferation of LUAD cells with different expression levels of OVOL2 by using colony formation (Figure 2B), EDU (5-ethynyl-2′-deoxyuridine) proliferation assay (Figure 2C) and CCK-8 assay (Figure 2D). The results showed that the OVOL2-knockdown group had a stronger proliferative ability. However, the proliferation ability was decreased after the overexpression of OVOL2. Real-time PCR was used to verify that OVOL2 knockdown increased the expression level of ki-67, which is a key protein of cell proliferation (Figures S3B and S3C; Table S3). Transwell assay (Figure 2E) and wound-healing assay (Figure 2F) in PC9 and A549 cells showed that OVOL2 knockdown promoted invasion and migration, when the upregulation of OVOL2 suppressed the migration and invasion abilities *in vitro*.

All these results suggest that the decrease in OVOL2 expression induces the proliferation, invasion, and metastasis of LUAD cells, which corroborates our previous analysis of clinical data showing that patients with LUAD with low OVOL2 expression levels have an increased likelihood of having increased tumor size, LN metastasis, and TNM stage (Figures 1I–1K).

Knockdown of OVOL2 promotes EMT in LUAD

To investigate further whether the proliferation and migration of LUAD cells regulated by OVOL2 are related to EMT, we used gene set enrichment analysis (GSEA) based on the TCGA database. The results indicated that OVOL2 expression was negatively correlated with EMT in LUAD (Figure 3A). Next, we analyzed the mRNA expression levels of OVOL2 in EMT-associated genes using the ENCORI database and found that OVOL2 was positively correlated with the epithelial phenotype E-cadherin (Figure 3B), but negatively correlated with the mesenchymal

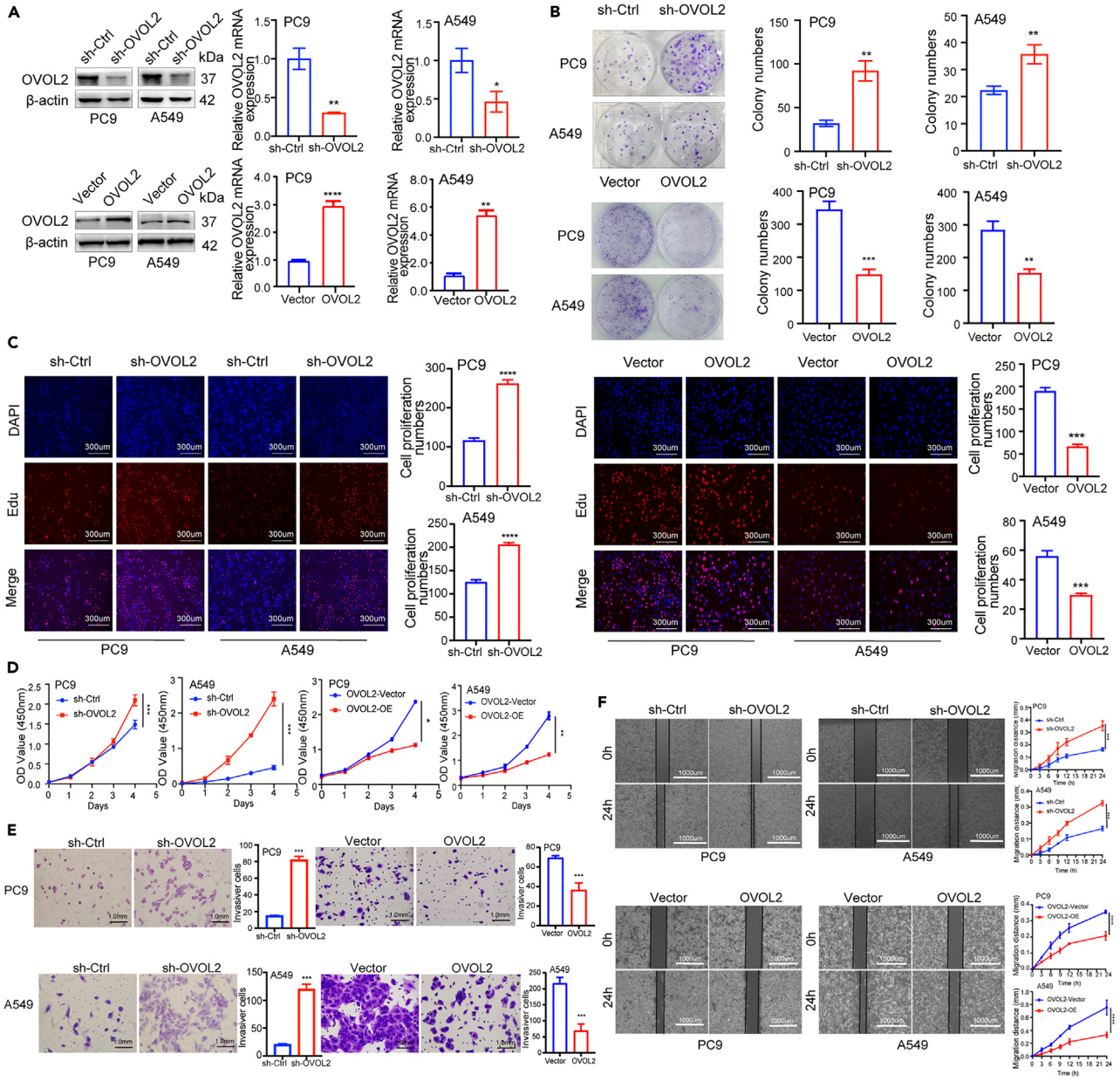

Figure 2. Knockdown of OVOL2 promotes LUAD cell proliferation, invasion, and migration *in vitro*

(A) The construction of the OVOL2 stable knockdown and overexpression in PC9 and A549 LUAD cell lines.

(B) Colony formation assay showing the effects of OVOL2 knockdown or overexpression in PC9 and A549 cell growth.

(C) EDU proliferation assay showing the proliferative abilities in knockdown and overexpression groups of PC9 and A549 cells.

(D) CCK-8 assay analysis of the impact of OVOL2 knockdown or overexpression on PC9 and A549 cell growth.

(E) The invasive ability of the OVOL2 knockdown or overexpression in the invasion assay.

(F) Wound-healing assay comparing the migration distance of OVOL2 knockdown or overexpression on PC9 and A549 cells. *$p < 0.05$, **$p < 0.01$, ***$p < 0.001$. Data were expressed as the mean ± SDs.

phenotypes vimentin, N-cadherin, TWIST1, ZEB1, SNAIL, and MMP9 (Figures 3C–3H). Furthermore, WB was used to verify that the knockdown of OVOL2 decreased E-cadherin and increased vimentin in PC9 and A549 cells (Figures 3I, S2F, and S2G). Conversely, OVOL2 overexpression showed the opposite effects on these proteins in PC9 and A549 cells (Figures 3J, S2H, and S2I). We also used the real-time PCR to verify that the knockdown of OVOL2 increased mesenchymal phenotypes, such as N-cadherin, MMP9, TWIST1, ZEB1, SNAIL, vimentin, and SLUG (Figures 3K and 3L, Table S3). All these results suggest that the knockdown of OVOL2 promoted EMT and that OVOL2 may regulate the malignant phenotypic transformation of LUAD cells.

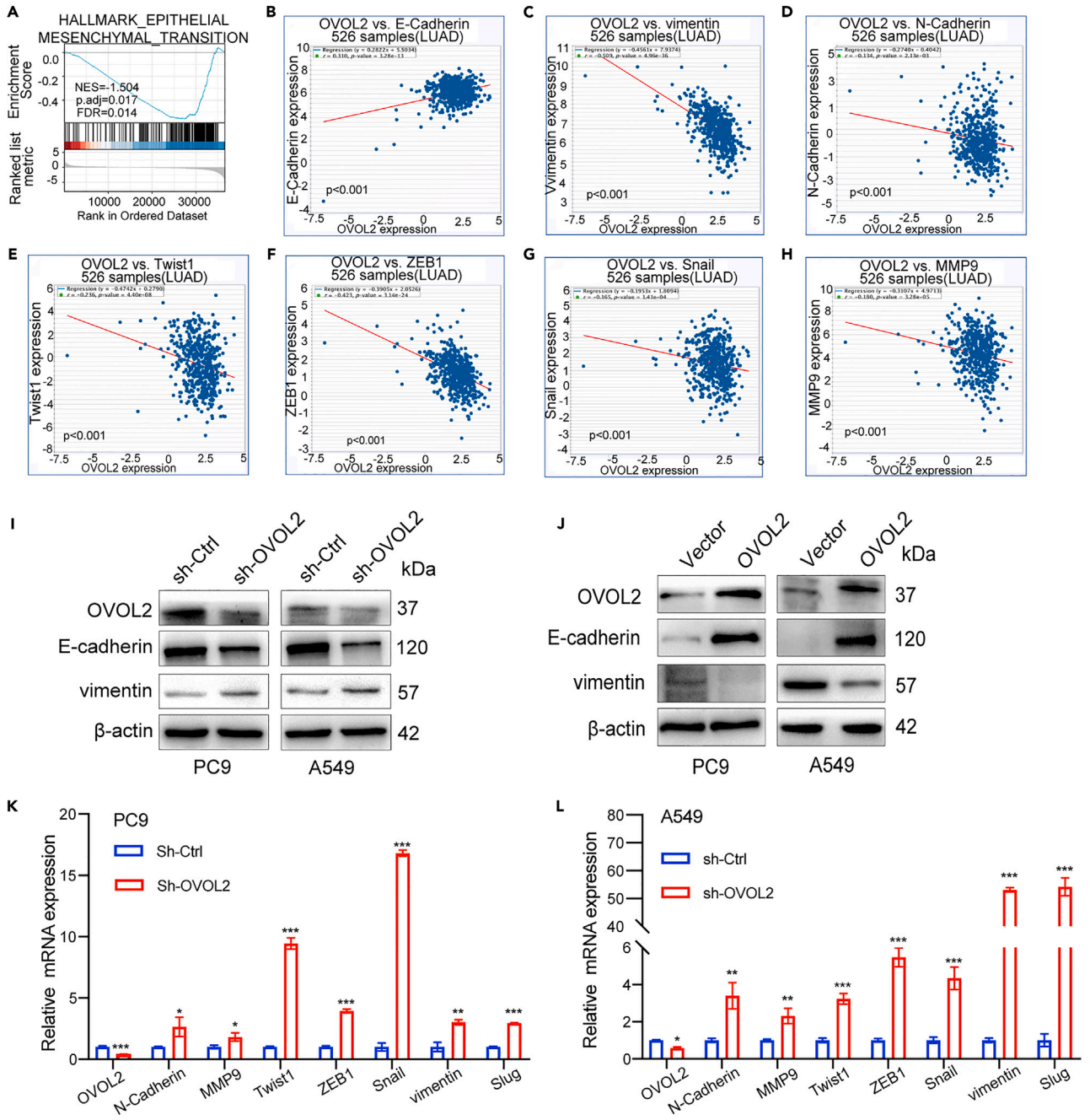

Figure 3. Knockdown of OVOL2 promotes EMT in LUAD

(A) GSEA validating the correlation between OVOL2 expression and epithelial-mesenchymal transition in LUAD.

(B) OVOL2 was positively correlated with epithelial phenotypes E-cadherin.

(C–H) OVOL2 was negatively correlated with mesenchymal phenotypes vimentin, N-cadherin, TWIST1, ZEB1, SNAIL, and MMP9.

(I and J) Western blotting analysis of EMT-related protein levels of OVOL2 knockdown and overexpression on PC9 and A549 LUAD cell lines.

(K and L) Real-timePCR analysis of EMT-related mRNA levels in PC9 and A549 cells. *p < 0.05, **p < 0.01, ***p < 0.001. Data were expressed as the mean ± SDs.

OVOL2 overexpression induces autolysosomal vacuolization

During the experiment, we found that many vacuoles appeared under the microscope in OVOL2-overexpressing cells (Figure 4A). Previous studies have reported that the vesicular structure of sh-NUPR1 lentivirus transfection in A549 cells may be acidic autophagy or lysosomes.[18] Thus, we boldly hypothesized that OVOL2 overexpression was associated with autophagic cancer cell death. To verify whether OVOL2 is involved in regulating autophagy, we first detected the expression of autophagy-related proteins by WB. Reduced OVOL2 expression

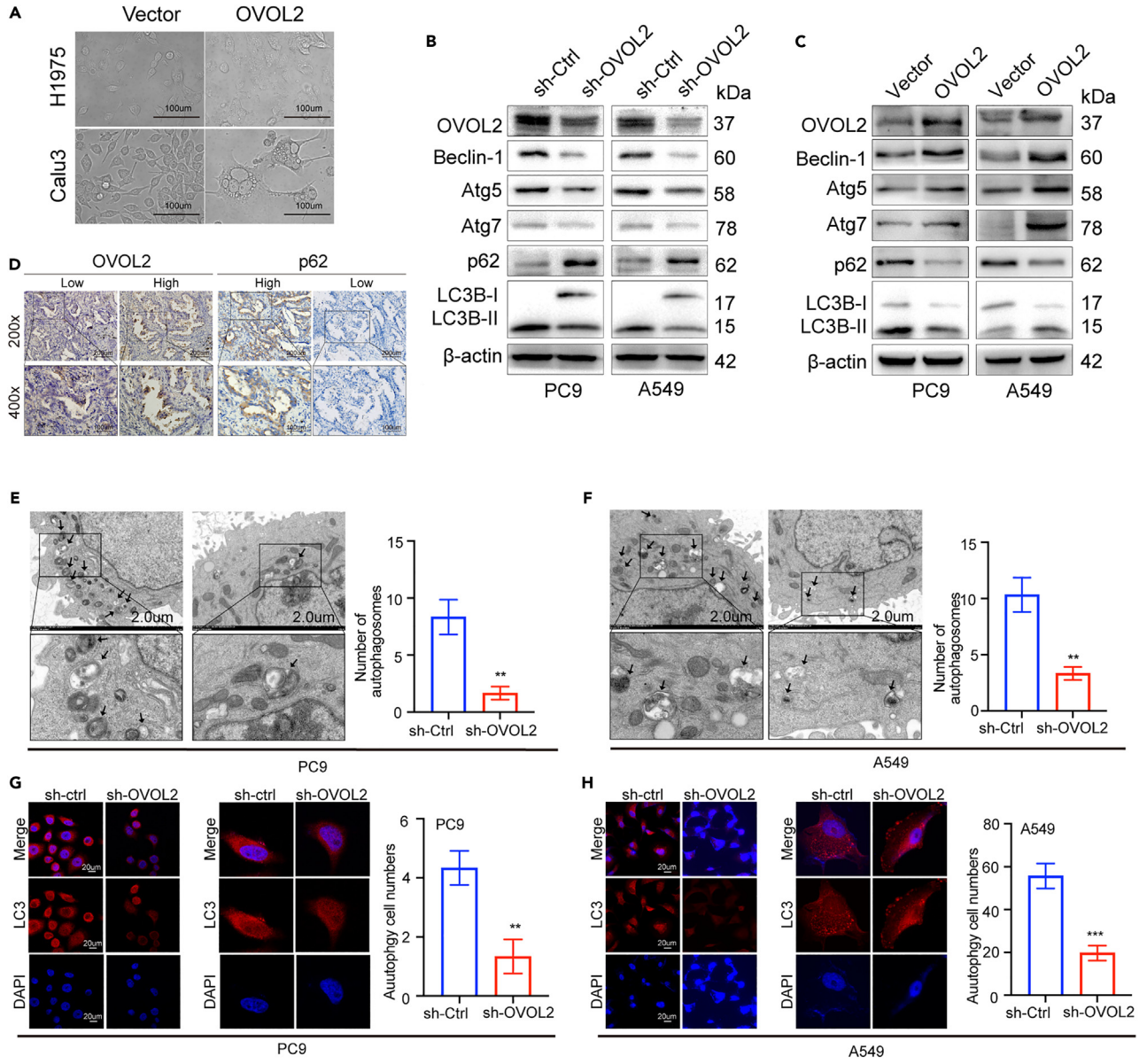

Figure 4. OVOL2-overexpression induces autolysosomal vacuolization

(A) Overexpression of OVOL2 induces a large number of vesicle-like structures in H1975 and Calu3 cells.

(B and C) Western blotting analysis of autophagy-related protein level of OVOL2 knockdown or overexpression in PC9 and A549 cells.

(D) Clinical specimens show OVOL2 and p62 protein expression via immunohistochemistry (IHC).

(E and F) Autophagy was evaluated using TEM in PC9 and A549 sh-Ctrl and sh-OVOL2 cells. The arrows indicate autophagosomes or autolysosomes. Scale bar: 2μm.

(G and H) PC9 sh-Ctrl, PC9 sh-OVOL2, A549 sh-Ctrl, and A549 sh-OVOL2 cells were immunostaining with antibodies against LC3B. Scale bar: 20μm.*$p < 0.05$, **$p < 0.01$, ***$p < 0.001$. Data were expressed as the mean ± SDs.

resulted in decreased levels of LC3B II, Beclin-1, Atg5 and Atg7 and increased levels of p62 (Figures 4B, S2J, and S2K), whereas OVOL2 overexpression showed the opposite effects on these proteins in PC9 and A549 cells (Figures 4C,S2L, and S2M). Next, we used 93 cases of LUAD samples, which tested for OVOL2 expression to examine p62 protein expression via IHC (Figure 4D). Besides, we also conducted a correlation analysis between OVOL2 and p62 based on the immunoreactivity score. The results showed that OVOL2 was negatively correlated with p62 expression (Figure S4E). Then we observed the number of autophagosomes in the PC9 and A549 sh-OVOL2 groups by transmission electronic microscopy. The results showed that the number of autophagosomes was decreased in sh-OVOL2 cells compared with control PC9 and A549 cells (Figures 4E and 4F). We also assessed autophagosomes by GFP-LC3B dot formation, and consistently, the results showed that the

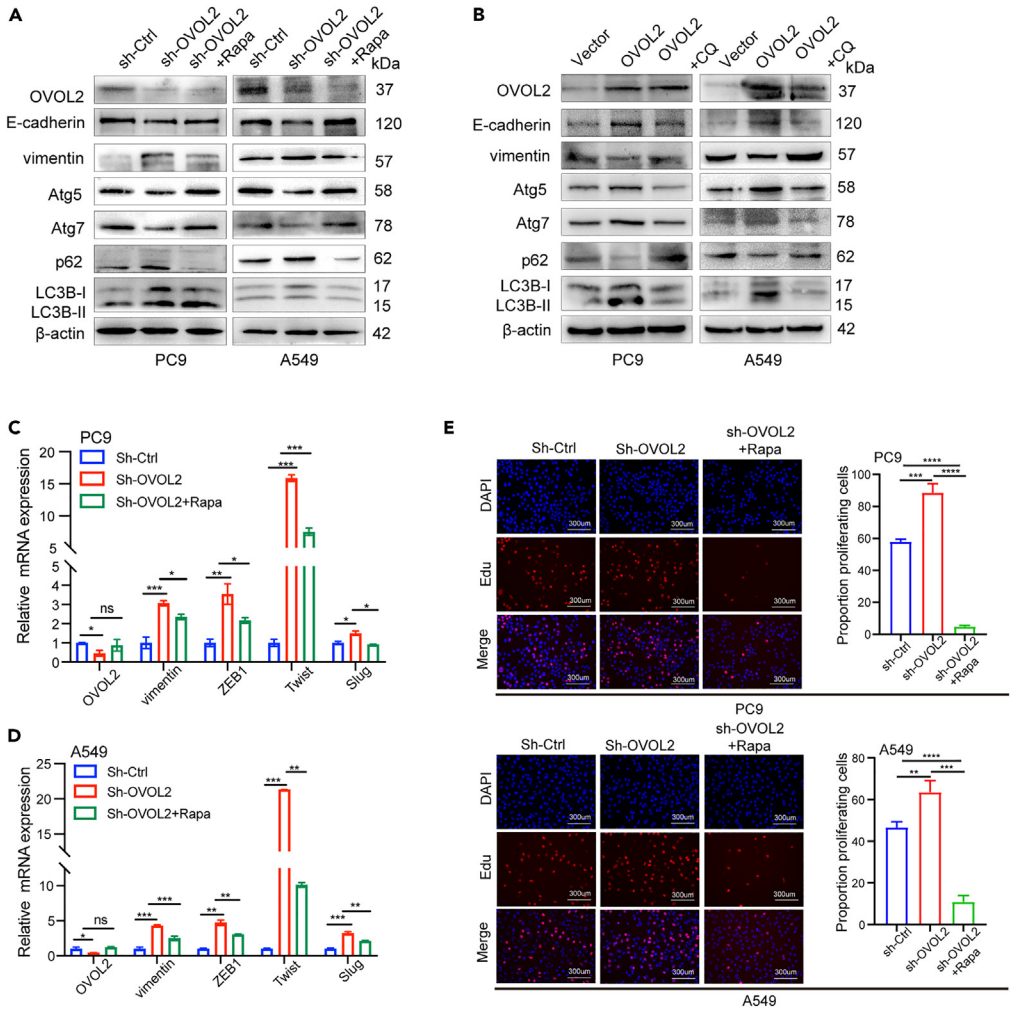

Figure 5. Knockdown of OVOL2 promoted EMT by inhibiting autophagy in the LUAD cell line

(A and B) Western blotting analysis of EMT and autophagy-related protein levels in PC9 and A549 cells.

(C and D) Real-time PCR analysis of mesenchymal phenotypes mRNA levels in PC9 and A549 cells.

(E) Sh-OVOL2 cells were pretreated with rapamycin. The cell proliferation activity was detected by EDU proliferation assay in sh-Ctrl, sh-OVOL2, and sh-OVOL2+rapamycin groups. *p < 0.05, **p < 0.01, ***p < 0.001. Data were expressed as the mean ± SDs.

number of GFP-LC3B dots in PC9 and A549 sh-OVOL2 cells was lower than that in sh-Ctrl cells (Figures 4G and 4H). These results indicated that the knockdown of OVOL2 inhibited autophagy in LUAD cells, which was confirmed from another aspect that the massive death of LUAD cells by overexpression of OVOL2 was responsible for the activation of autophagy.

Autophagy inhibited by knockdown of OVOL2 promotes EMT in LUAD cells

Several studies have shown that autophagy may play an important role in the regulation of EMT.[10,19] To determine whether OVOL2-mediated autophagy is associated with EMT in LUAD cells, we used rapamycin and CQ to activate and inhibit autophagy, respectively. When we treated OVOL2 knockdown cells with rapamycin to activate autophagy, EMT-related proteins changed accordingly. WB results showed that epithelial phenotypes increased E-cadherin, which was originally suppressed. The mesenchymal phenotype vimentin was decreased, which was originally increased (Figures 5A, S2N, and S2O). Meanwhile, when OVOL2-overexpressed cells were treated with CQ to inhibit autophagy, WB showed the opposite effects on these proteins in LUAD PC9 and A549 cells (Figures 5B, S2P, and S2Q). Real-time PCR results showed that after rapamycin-activated autophagy in OVOL2 knockdown cells, the mRNA levels of vimentin, ZEB1, TWIST, and SLUG were reduced (Figures 5C and 5D).

Additionally, we re-tested cell proliferation activity under sh-OVOL2 conditions in co-treatment with rapamycin, and cell proliferation activity changed accordingly. Remarkably, rapamycin treatment significantly inhibited cell proliferation activity, which was initially strengthened

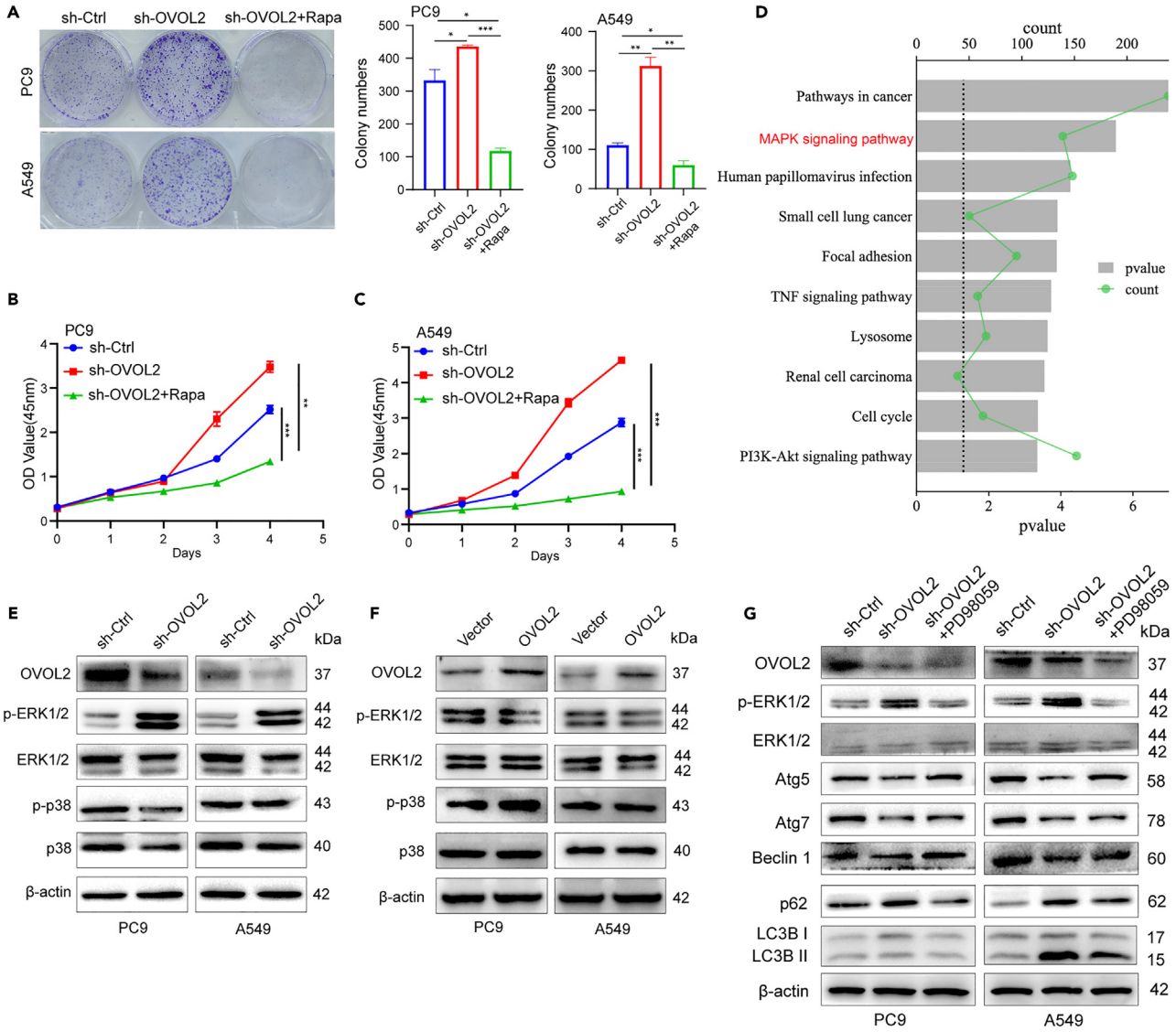

Figure 6. Knockdown of OVOL2 inhibited cell autophagy through the MAPK signaling pathway in LUAD

(A) Plate clone formation assay assessed the cell proliferation activity in sh-Ctrl, sh-OVOL2, and sh-OVOL2+rapamycin groups.

(B and C) The cell proliferation activity was detected by CCK-8 assay in sh-Ctrl, sh-OVOL2, and sh-OVOL2+rapamycin groups.

(D) Signal pathway enrichment analysis of TCGA database by RNA-seq.

(E and F) The effect of the downregulation and upregulation of OVOL2 expression on MAPK signaling pathway activation was verified by western blotting in PC9 and A549 cells.

(G) Sh-OVOL2 cells were pretreated with PD98059. Western blotting analysis of the protein levels of *p*-ERK1/2, ERK1/2, and autophagy-related protein. *$p < 0.05$, **$p < 0.01$, ***$p < 0.001$. Data were expressed as the mean ± SDs.

in OVOL2 knock-down cells by EDU proliferation assay, plate clone formation assay (Figures 5E and 6A), and CCK-8 assay (Figures 6B and 6C). On the contrary, when we treated OVOL2 overexpression cells with CQ to inhibit autophagy activity, CQ treatment significantly strengthened cell proliferation, which was initially inhibited in OVOL2 overexpression cells by CCK8 assay(Figures S4A and S4B), plate clone formation assay (Figure S4C). Meanwhile, we re-tested cell invasion activity under sh-OVOL2 conditions in co-treat with rapamycin. Accordingly, rapamycin treatment significantly inhibited cell invasion activity, which was initially strengthened in OVOL2 knock-down cells by transwell assay (Figure S4D). Taken together, these results indicated that the knockdown of OVOL2 promoted EMT by inhibiting autophagy in the LUAD cell line.

Knockdown of OVOL2 inhibits cell autophagy via the MAPK signaling pathway in LUAD

To demonstrate further the downstream molecular mechanism of OVOL2, we used GSEA software to explore some related signaling pathways. Pathway enrichment was performed on the basis of differentially expressed genes. Notably, in addition to genes in pathways involved in

cancer, genes in the MAPK signaling pathway were significantly enriched (Figure 6D and Table S5). Next, WB revealed that downregulated OVOL2 expression strengthens the protein level of *p*-ERK1/2 in PC9 and A549 cells. However, the protein level of p-p38 did not change significantly (Figures 6E, 6F, and S2R–S2U). To investigate the relationship between the MAPK pathway and autophagy, we treated PC9 and A549 OVOL2 knockdown cells with PD98059, an MEK/ERK inhibitor. *p*-ERK1/2 expression was significantly increased in sh-OVOL2 cells but was effectively suppressed upon treatment with PD98059. WB further showed that the PD98059-mediated inhibition of *p*-ERK1/2 significantly attenuated the levels of the autophagy-related proteins Atg5, Atg7, Beclin1, and LC3B I-II and increased the levels of p62 in sh-OVOL2 cells (Figures 6G, S2V, and S2W). All these results indicated that OVOL2 regulated autophagy in LUAD cells through the ERK1/2 MAPK signaling pathway.

DISCUSSION

Previous studies have confirmed that OVOL2 plays an important role in tumor development and metastasis.[20–22] In our study, we first found that the expression level of OVOL2 was significantly reduced in LUAD tumor tissues and negatively correlated with the OS and DFS of patients with LUAD using a large-scale LUAD tissue microarray. Low OVOL2 expression was an independent risk factor in patients with LUAD that had poor prognosis and was significantly associated with clinicopathological features, such as tumor size, LN metastasis, and TNM stage. Surprisingly, in contrast to patients with LUSC, those with LUAD showed a detectable correlation between OVOL2 expression and prognosis. This correlation is the first evidence of the significance of OVOL2 in LUAD, and OVOL2 may be used as a specific biomarker and target in LUAD. The reason for this result may be that although LUAD and LUSC are histologically classified as NSCLC, significant differences were found in their molecular composition, response to systemic treatment strategies and survival prognosis.[23,24] In addition, significant differences were found between LUAD and LUSC in gene expression and microbial abundance associated with recurrence and metastasis.[25]

The occurrence and development of tumors are closely related to biological processes, including EMT and autophagy.[26] EMT is the mechanism most closely associated with tumor cell invasion and metastasis and is characterized by morphological and physiological changes, such as loss of cell polarity, disruption of intracellular junctions, and increased growth and invasion.[27] Multiple studies have shown that OVOL2, as a transcription factor, inhibits EMT in tumor cells.[22,28,29] This result is consistent with our research results. In the current work, the downregulation of OVOL2 promoted cell proliferation, migration, invasion, and EMT. Autophagy is a type of programmed cell death that is known to play a dual role in cancer, acting as a cytoprotective or cytotoxic mechanism and playing a pivotal role in the tumor metastatic process.[30] At the same time, dysregulated autophagy plays a key role in cancer cell survival and death and is therefore gaining increasing attention in cancer therapy.[31,32] In particular, in advanced cancer, enhancing and inhibiting autophagy have been proposed as therapeutic strategies,[33,34] and induction or inhibition of autophagy contributes to the efficacy of immunotherapy.[35] In this study, we showed that the downregulation of OVOL2 affected the downstream autophagy-related markers Beclin-1, p62, Atg5, Atg7, and LC3B. Most importantly, when we established OVOL2 overexpression cell lines, several LUAD cell lines, such as H1975, Calu3, HCC827, and H1299, were used, resulting in significant cell death and preventing the establishment of stable overexpression cell lines. We concluded that the reason for cell death may be excessive autophagy. The knockdown of OVOL2 resulted in decreased autophagy levels, indicating that the overexpression of OVOL2 promotes autophagy and leads to significant LUAD cell death.

The relationship between autophagy and EMT is complex. Emerging evidence has shown that EMT and cancer metastasis are directly correlated with autophagy.[36] Elucidating the crosstalk between autophagy and EMT may provide new targets for cancer treatment. However, whether autophagy promotes or inhibits EMT remains arguable. On the one hand, some studies have suggested that stimulated autophagy promotes the occurrence of EMT in hepatocellular carcinoma cells.[37] On the other hand, some studies have shown that autophagy inhibits the occurrence of EMT in gastric cancer cells.[38] Autophagy can also reverse EMT by reducing key proteins, such as SNAIL, SLUG, and TWIST in human glioblastoma cells.[39] To date, several studies have demonstrated that tumor cells can use EMT or autophagy in response to microenvironmental stress, that EMT and autophagy negatively regulate each other and that they are capable of interconversion.[40,41] In this study, we confirmed that OVOL2-mediated autophagy is associated with EMT in LUAD cells. We performed a series of experiments to clarify this point. We used Atg5, Atg7, LC3B-I/II, and p62 as autophagy markers; E-cadherin as an epithelial phenotype marker; and vimentin as an interstitial phenotype marker. When we stimulated downregulated OVOL2 cells with rapamycin (an autophagy activator), OVOL2 knockdown-induced LUAD cell EMT-related proteins E-cadherin and vimentin were rescued. On the contrary, when we used an autophagy inhibitor chloroquine (CQ) to inhibit autophagy in OVOL2 overexpression cells, EMT-related proteins changed accordingly. Here, we report for the first time the possible interaction between autophagy and EMT mediated by OVOL2 and its consequences in cancer metastasis.

To investigate the mechanism underlying how OVOL2 regulates autophagy in LUAD cells, GSEA was used for KEGG pathway enrichment analysis. The results showed that genes in the MAPK signaling pathway were significantly enriched. ERK1/2, p38, and JNK are the three most abundant subfamilies of MAPK. Among them, ERK1/2 MAPK is mainly involved in lung cell death, pathogenesis, development, carcinogenic activity, and the growth of lung cancer cells.[42–45] In addition, the ERK1/2 MAPK signaling pathway may be an important pathway of autophagy in cancer.[46–48] In the present study, we found that *p*-ERK1/2 expression changed with OVOL2 expression but not p-p38 expression. When we stimulated downregulated OVOL2 cells with PD98059 (an ERK/MEK inhibitor), the OVOL2 knockdown-inhibited LUAD cell autopsy was rescued. However, this part of the research still has several limitations. Firstly, further molecular biology experiments are needed to explore the underlying mechanism (such as the interaction) of the activation of the ERK1/2 MAPK and EMT signaling pathways induced by the upregulation of OVOL2. Second, previous studies of OVOL2 in LUAD progression, especially its correlation with the ERK1/2 MAPK pathway, were limited, thus also limiting our exploration of the molecular mechanism to some extent. Therefore, our findings may initially provide a basis for further studies to explore the downstream mechanism of OVOL2 expression-induced LUAD progression.

Conclusions

In conclusion, we confirmed that OVOL2 expression was lower in LUAD and that patients with low OVOL2 expression had a worse prognosis. OVOL2 may serve as a specific prognostic biomarker in patients with LUAD. Our study demonstrated for the first time that OVOL2 induces autophagy-mediated EMT through ERK1/2 MAPK signaling. All these data highlight the biological functions of OVOL2 and the novel OVOL2-mediated mechanism, which may be a new target for LUAD therapy.

Limitations of the study

There are some limitations in our study. Firstly, in this study, only 93 LUAD cases were included, which is not sufficient to allow a larger comparative assessment. Therefore, future experiments should examine more samples. Second, current research is insufficient in time and funding to complement *in vivo* experiments. It should be pointed out that, this exclusion does not undermine the fundamental premise of the research. However, animal models will be further improved in future research.

STAR★METHODS

Detailed methods are provided in the online version of this paper and include the following:

- KEY RESOURCES TABLE
- RESOURCE AVAILABILITY
  - Lead contact
  - Materials availability
  - Data and code availability
- EXPERIMENTAL MODEL AND STUDY PARTICIPANT DETAILS
  - Clinical samples
  - Cell line and cell culture
- METHOD DETAILS
  - Immunohistochemistry
  - Cell viability assay
  - Colony formation assay
  - Wound healing assay
  - Invasion assay
  - Transfection assay
  - Fluorescence microscopy and confocal microscopy
  - Transmission electron microscopy
- QUANTIFICATION AND STATISTICAL ANALYSIS

SUPPLEMENTAL INFORMATION

Supplemental information can be found online at https://doi.org/10.1016/j.isci.2024.108873.

ACKNOWLEDGMENTS

We are grateful for the financial support from the Key Project of Science and Technology Research in Universities of Inner Mongolia (China) (No.NJZZ22162); The Health Science and Technology Plan Class A Project of Inner Mongolia (China) (No.202201552); Key Project of Science & Technology Development Fund of Tianjin Education Commission for Higher Education (China) (No.2022ZD064); and Tianjin Key Medical Discipline(Specialty) Construction Project (China) (TJYXZDXK-010A).

AUTHOR CONTRIBUTIONS

H.G., P.C., and Y.W. conceived the idea and designed the experiments. Y.W. and L.S. performed experiments and analyzed and interpreted the data. Y.W., H.G., and Y.H. wrote and revised the paper. W.G., Y.C., R.Z., Y.W., Y.L., L.C., and Z.L. participated in part of the experiments.

DECLARATION OF INTERESTS

The authors declare no competing interests.

Received: August 11, 2023
Revised: November 28, 2023
Accepted: January 8, 2024
Published: January 11, 2024

REFERENCES

1. Siegel, R.L., Miller, K.D., Fuchs, H.E., and Jemal, A. (2022). Cancer statistics, CA Cancer. J Clin *72*, 7–33.
2. Boch, T., Köhler, J., Janning, M., and Loges, S. (2022). Targeting the EGF receptor family in non-small cell lung cancer-increased complexity and future perspectives. Cancer Biol. Med. *19*, 1543–1564.
3. Thai, A.A., Solomon, B.J., Sequist, L.V., Gainor, J.F., and Heist, R.S. (2021). Lung cancer. Lancet *398*, 535–554.
4. Succony, L., Rassl, D.M., Barker, A.P., McCaughan, F.M., and Rintoul, R.C. (2021). Adenocarcinoma spectrum lesions of the lung: Detection, pathology and treatment strategies. Cancer Treat Rev. *99*, 102237.
5. Chen, Y., Xia, L., Peng, Y., Wang, G., Bi, L., Xiao, X., Li, C., and Li, W. (2022). Development and validation of a m^{6}A -regulated prognostic signature in lung adenocarcinoma. Front. Oncol. *12*, 947808.
6. Gundamaraju, R., Lu, W., Paul, M.K., Jha, N.K., Gupta, P.K., Ojha, S., Chattopadhyay, I., Rao, P.V., and Ghavami, S. (2022). Autophagy and EMT in cancer and metastasis: Who controls whom? Biochim. Biophys. Acta, Mol. Basis Dis. *1868*, 166431.
7. Li, D., Xia, L., Huang, P., Wang, Z., Guo, Q., Huang, C., Leng, W., and Qin, S. (2023). Heterogeneity and plasticity of epithelial-mesenchymal transition (EMT) in cancer metastasis: Focusing on partial EMT and regulatory mechanisms. Cell Prolif. *56*, e13423.
8. Dower, C.M., Wills, C.A., Frisch, S.M., and Wang, H.G. (2018). Mechanisms and context underlying the role of autophagy in cancer metastasis. Autophagy *14*, 1110–1128.
9. Qiang, L., Zhao, B., Ming, M., Wang, N., He, T.C., Hwang, S., Thorburn, A., and He, Y.Y. (2014). Regulation of cell proliferation and migration by p62 through stabilization of Twist1. Proc. Natl. Acad. Sci. USA *111*, 9241–9246.
10. Zheng, B., Song, K., Sun, L., Gao, Y., Qu, Y., Ren, C., Yan, P., Chen, W., Guo, W., Zhou, C., and Yue, B. (2022). Siglec-15-induced autophagy promotes invasion and metastasis of human osteosarcoma cells by activating the epithelial-mesenchymal transition and Beclin-1/ATG14 pathway. Cell Biosci. *12*, 109.
11. Qiang, L., and He, Y.Y. (2014). Autophagy deficiency stabilizes TWIST1 to promote epithelial-mesenchymal transition. Autophagy *10*, 1864–1865.
12. Li, B., Dai, Q., Li, L., Nair, M., Mackay, D.R., and Dai, X. (2002). Ovol2, a mammalian homolog of Drosophila ovo: gene structure, chromosomal mapping, and aberrant expression in blind-sterile mice. Genomics *80*, 319–325.
13. Jeyarajah, M.J., Jaju Bhattad, G., Hillier, D.M., and Renaud, S.J. (2020). The Transcription Factor OVOL2 Represses ID2 and Drives Differentiation of Trophoblast Stem Cells and Placental Development in Mice. Cells *9*, 840.
14. Saxena, K., Srikrishnan, S., Celia-Terrassa, T., and Jolly, M.K. (2022). OVOL1/2: Drivers of Epithelial Differentiation in Development, Disease, and Reprogramming. Cells Tissues Organs *211*, 183–192.
15. Xia, L., Gao, J., Ma, K., Lin, H., Chen, Y., Luo, Q., and Lian, J. (2021). OVOL2 attenuates the expression of MAP3K8 to suppress epithelial mesenchymal transition in colorectal cancer. Pathol. Res. Pract. *224*, 153493.
16. Murata, M., Ito, T., Tanaka, Y., Yamamura, K., Furue, K., and Furue, M. (2020). OVOL2-Mediated ZEB1 Downregulation May Prevent Promotion of Actinic Keratosis to Cutaneous Squamous Cell Carcinoma. J. Clin. Med. *9*, 618.
17. Liu, J., Wu, Q., Wang, Y., Wei, Y., Wu, H., Duan, L., Zhang, Q., and Wu, Y. (2018). Ovol2 induces mesenchymal-epithelial transition via targeting ZEB1 in osteosarcoma. OncoTargets Ther. *11*, 2963–2973.
18. Mu, Y., Yan, X., Li, D., Zhao, D., Wang, L., Wang, X., Gao, D., Yang, J., Zhang, H., Li, Y., et al. (2018). NUPR1 maintains autolysosomal efflux by activating SNAP25 transcription in cancer cells. Autophagy *14*, 654–670.
19. Liu, X., Meng, L., Li, X., Li, D., Liu, Q., Chen, Y., Li, X., Bu, W., and Sun, H. (2020). Regulation of FN1 degradation by the p62/SQSTM1-dependent autophagy-lysosome pathway in HNSCC. Int. J. Oral Sci. *12*, 34.
20. Zhang, X., Luo, F., Luo, S., Li, L., Ren, X., Lin, J., Liang, Y., Ma, C., Ding, L., Zhang, D., et al. (2022). Transcriptional Repression of Aerobic Glycolysis by OVOL2 in Breast Cancer. Adv. Sci. *9*, e2200705.
21. Zhang, R., Geng, G.J., Guo, J.G., Mi, Y.J., Zhu, X.L., Li, N., Liu, H.M., Lin, J.F., Wang, J.W., Zhao, G., et al. (2022). An NF-κB/OVOL2 circuit regulates glucose import and cell survival in non-small cell lung cancer. Cell Commun. Signal. *20*, 40.
22. Gugnoni, M., Manzotti, G., Vitale, E., Sauta, E., Torricelli, F., Reggiani, F., Pistoni, M., Piana, S., and Ciarrocchi, A. (2022). OVOL2 impairs RHO GTPase signaling to restrain mitosis and aggressiveness of Anaplastic Thyroid Cancer. J. Exp. Clin. Cancer Res. *41*, 108.
23. Fukuoka, M., Wu, Y.L., Thongprasert, S., Sunpaweravong, P., Leong, S.S., Sriuranpong, V., Chao, T.Y., Nakagawa, K., Chu, D.T., Saijo, N., et al. (2011). Biomarker analyses and final overall survival results from a phase III, randomized, open-label, first-line study of gefitinib versus carboplatin/paclitaxel in clinically selected patients with advanced non-small-cell lung cancer in Asia (IPASS). J. Clin. Oncol. *29*, 2866–2874.
24. Zengin, T., and Önal-Süzek, T. (2021). Comprehensive Profiling of Genomic and Transcriptomic Differences between Risk Groups of Lung Adenocarcinoma and Lung Squamous Cell Carcinoma. J. Personalized Med. *11*, 154.
25. Zhou, X., Ji, L., Ma, Y., Tian, G., Lv, K., and Yang, J. (2023). Intratumoral Microbiota-Host Interactions Shape the Variability of Lung Adenocarcinoma and Lung Squamous Cell Carcinoma in Recurrence and Metastasis. Microbiol. Spectr. *11*, e0373822.
26. Su, Z., Yang, Z., Xu, Y., Chen, Y., and Yu, Q. (2015). Apoptosis, autophagy, necroptosis, and cancer metastasis. Mol. Cancer *14*, 48.
27. Hashemi, M., Nadafzadeh, N., Imani, M.H., Rajabi, R., Ziaolhagh, S., Bayanzadeh, S.D., Norouzi, R., Rafiei, R., Koohpar, Z.K., Raei, B., et al. (2023). Targeting and regulation of autophagy in hepatocellular carcinoma: revisiting the molecular interactions and mechanisms for new therapy approaches. Cell Commun. Signal. *21*, 32.
28. Xie, C., Liu, G., Li, M., Fang, Y., Qian, K., Tang, Y., Wu, X., Lei, X., Li, X., Liu, Q., et al. (2019). Targeting TRPV1 on cellular plasticity regulated by Ovol 2 and Zeb 1 in hepatocellular carcinoma. Biomed. Pharmacother. *118*, 109270.
29. Sun, P., Han, Y., Plikus, M., and Dai, X. (2021). Altered Epithelial-mesenchymal Plasticity as a Result of Ovol2 Deletion Minimally Impacts the Self-renewal of Adult Mammary Basal Epithelial Cells. J. Mammary Gland Biol. Neoplasia *26*, 377–386.
30. Rahman, M.A., Saikat, A.S.M., Rahman, M.S., Islam, M., Parvez, M.A.K., and Kim, B. (2023). Recent Update and Drug Target in Molecular and Pharmacological Insights into Autophagy Modulation in Cancer Treatment and Future Progress. Cells *12*, 458.
31. Yamamoto, K., Venida, A., Yano, J., Biancur, D.E., Kakiuchi, M., Gupta, S., Sohn, A.S.W., Mukhopadhyay, S., Lin, E.Y., Parker, S.J., et al. (2020). Autophagy promotes immune evasion of pancreatic cancer by degrading MHC-I. Nature *581*, 100–105.
32. Liu, K., Lee, J., Kim, J.Y., Wang, L., Tian, Y., Chan, S.T., Cho, C., Machida, K., Chen, D., and Ou, J.H.J. (2017). Mitophagy Controls the Activities of Tumor Suppressor p53 to Regulate Hepatic Cancer Stem Cells. Mol. Cell *68*, 281–292.e5.
33. Levy, J.M.M., Towers, C.G., and Thorburn, A. (2017). Targeting autophagy in cancer. Nat. Rev. Cancer *17*, 528–542.
34. Jain, V., Singh, M.P., and Amaravadi, R.K. (2023). Recent advances in targeting autophagy in cancer. Trends Pharmacol. Sci. *44*, 290–302.
35. Lei, Y., Zhang, E., Bai, L., and Li, Y. (2022). Autophagy in Cancer Immunotherapy. Cells *11*, 2996.
36. Zada, S., Hwang, J.S., Ahmed, M., Lai, T.H., Pham, T.M., Elashkar, O., and Kim, D.R. (2021). Cross talk between autophagy and oncogenic signaling pathways and implications for cancer therapy. Biochim. Biophys. Acta Rev. Canc *1876*, 188565.
37. Hashemi, M., Sabouni, E., Rahmanian, P., Entezari, M., Mojtabavi, M., Raei, B., Zandieh, M.A., Behroozaghdam, M., Mirzaei, S., Hushmandi, K., et al. (2023). Deciphering STAT3 signaling potential in hepatocellular carcinoma: tumorigenesis, treatment resistance, and pharmacological significance. Cell. Mol. Biol. Lett. *28*, 33.
38. Wei, R., Xiao, Y., Song, Y., Yuan, H., Luo, J., and Xu, W. (2019). FAT4 regulates the EMT and autophagy in colorectal cancer cells in part via the PI3K-AKT signaling axis. J. Exp. Clin. Cancer Res. *38*, 112.
39. Yang, H.L., Chang, Y.H., Pandey, S., Bhat, A.A., Vadivalagan, C., Lin, K.Y., and Hseu, Y.C. (2023). Antrodia camphorata and coenzyme Q_0 , a novel quinone derivative of Antrodia camphorata, impede HIF-1α and epithelial-mesenchymal transition/metastasis in human glioblastoma cells. Environ. Toxicol. *38*, 1548–1564.
40. Coelho, B.P., Fernandes, C.F.d.L., Boccacino, J.M., Souza, M.C.D.S., Melo-Escobar, M.I., Alves, R.N., Prado, M.B., Iglesia, R.P., Cangiano, G., Mazzaro, G.L.R., and Lopes, M.H. (2020). Multifaceted WNT Signaling at the Crossroads Between Epithelial-Mesenchymal Transition and Autophagy in Glioblastoma. Front. Oncol. *10*, 597743.
41. Gugnoni, M., Sancisi, V., Manzotti, G., Gandolfi, G., and Ciarrocchi, A. (2016). Autophagy and epithelial-mesenchymal transition: an intricate interplay in cancer. Cell Death Dis. *7*, e2520.

42. Jain, A.S., Prasad, A., Pradeep, S., Dharmashekar, C., Achar, R.R., Ekaterina, S., Victor, S., Amachawadi, R.G., Prasad, S.K., Pruthvish, R., et al. (2021). Everything Old Is New Again: Drug Repurposing Approach for Non-Small Cell Lung Cancer Targeting MAPK Signaling Pathway. Front. Oncol. *11*, 741326.
43. Wang, C., Wen, M., Xu, J., Gao, P., Liu, S., Liu, J., Chen, Y., and Zhou, L. (2023). GTSE1 promotes the growth of NSCLC by regulating microtubule-associated proteins through the ERK/MAPK pathway. Thorac. Cancer *14*, 1624–1634.
44. Wei, C.H., Wu, G., Cai, Q., Gao, X.C., Tong, F., Zhou, R., Zhang, R.G., Dong, J.H., Hu, Y., and Dong, X.R. (2017). MicroRNA-330-3p promotes cell invasion and metastasis in non-small cell lung cancer through GRIA3 by activating MAPK/ERK signaling pathway. J. Hematol. Oncol. *10*, 125.
45. Liu, C., Li, H., Jia, J., Ruan, X., Liu, Y., and Zhang, X. (2019). High Metastasis-Associated Lung Adenocarcinoma Transcript 1 (MALAT1) Expression Promotes Proliferation, Migration, and Invasion of Non-Small Cell Lung Cancer via ERK/Mitogen-Activated Protein Kinase (MAPK) Signaling Pathway. Med. Sci. Mon. Int. Med. J. Exp. Clin. Res. *25*, 5143–5149.
46. Xiong, Q., Liu, A., Ren, Q., Xue, Y., Yu, X., Ying, Y., Gao, H., Tan, H., Zhang, Z., Li, W., et al. (2020). Cuprous oxide nanoparticles trigger reactive oxygen species-induced apoptosis through activation of erk-dependent autophagy in bladder cancer. Cell Death Dis. *11*, 366.
47. Stalnecker, C.A., Grover, K.R., Edwards, A.C., Coleman, M.F., Yang, R., DeLiberty, J.M., Papke, B., Goodwin, C.M., Pierobon, M., Petricoin, E.F., et al. (2022). Concurrent Inhibition of IGF1R and ERK Increases Pancreatic Cancer Sensitivity to Autophagy Inhibitors. Cancer Res. *82*, 586–598.
48. Yuan, J., Dong, X., Yap, J., and Hu, J. (2020). The MAPK and AMPK signalings: interplay and implication in targeted cancer therapy. J. Hematol. Oncol. *13*, 113.

STAR★METHODS

KEY RESOURCES TABLE

REAGENT or RESOURCE	SOURCE	IDENTIFIER
Antibodies		
Anti-OVOL2 antibody	Abcam	Cat# ab169469; RRID:AB_3083579
Anti-beta Actin antibody	Abcam	Cat# ab8227; RRID:AB_2305186
Anti-APG5L/ATG5 antibody [EPR1755(2)]	Abcam	Cat# ab108327; RRID:AB_2650499
Anti-ATG7 antibody [EP1759Y]	Abcam	Cat# ab52472; RRID:AB_867756
Anti-Beclin-1 antibody [EPR19662]	Abcam	Cat# ab302669; RRID:AB_3083581
Anti-SQSTM1/p62 antibody [EPR18351]	Abcam	Cat# ab207305; RRID:AB_2885112
Anti-Vimentin antibody [EPR3776]	Abcam	Cat# ab92547; RRID:AB_10562134
Phospho-p44/42 MAPK (Erk1/2)	Cell Signaling technology	Cat#4370; RRID: AB_2315112
LC3B (D11)	Cell Signaling technology	Cat#3868; RRID: AB_2137707
Phospho-p38 MAPK	Cell Signaling technology	Cat#4511 ; RRID:AB_2139682
p44/42 MAPK (Erk1/2) (137F5)	Cell Signaling technology	Cat#4695; RRID:AB_390779
p38 MAPK (D13E1)	Cell Signaling technology	Cat#8690; RRID:AB_10999090
E-Cadherin (24E10)	Cell Signaling technology	Cat#3195; RRID:AB_2291471
Biological samples		
Human Lung cancer tissue	Tianjin Medical University Cancer Institute and Hospital (Tianjin, China)	N/A
Human Lung tissue	Tianjin Medical University Cancer Institute and Hospital (Tianjin, China)	N/A
Chemicals, peptides, and recombinant proteins		
PD98059	MedChemExpress	Cat# HY-12028
Rapamycin (Sirolimus)	Selleck	Cat# S1039
Chloroquine(CQ)	Selleck	Cat# S6999
RPMI-1640	Gibco	Cat# 11875101
Critical commercial assays		
CCK-8 Cell Proliferation and Cytotoxicity Assay Kit	Solarbio	Cat# CA1210
BeyoClick™ EdU Cell Proliferation Kit with Alexa Fluor 488	Beyotime	Cat# C0071
Deposited data		
TCGA database	The Genomic Data Commons (GDC)	https://portal.gdc.cancer.gov/
Experimental models: Cell lines		
Human cell line: A549	Gift from Yi Luo	N/A
Human cell line: PC9	Gift from Yi Luo	N/A
Human cell line: Calu3	Gift from Yi Luo	N/A
Human cell line: H1975	Gift from Yi Luo	N/A
Human cell line: HEK293T	N/A	N/A
Oligonucleotides		
Primers for qPCR, see Table S1	This study	N/A
Software and algorithms		
ImageJ (Fiji)	ImageJ Software	N/A
GraphPad Prism7	GraphPad Software	N/A
R 4.2.1	The R Foundation for Statistical Computing	https://www.r-project.org/

RESOURCE AVAILABILITY

Lead contact

For further information and requests for resources, please contact Hua Guo (guohua@tjmuch.com).

Materials availability

This study did not generate new unique reagents.

Data and code availability

- Data reported in this paper will be shared by the lead contact upon request.
- This paper does not report original code.
- Any additional information required to reanalyze the data reported in this paper is available from the lead contact upon request.

EXPERIMENTAL MODEL AND STUDY PARTICIPANT DETAILS

Clinical samples

Human LUAD, lung squamous cell carcinoma (LUSC) and adjacent nonmalignant tissue samples were obtained from the Tianjin Medical University Cancer Institute and Hospital (Tianjin, China) between January 2007 and December 2010. None of the patients had undergone adjuvant therapy, such as radiotherapy or chemotherapy, before surgical resection. All tissue samples were verified to be LUAD, LUSC or adjacent normal tissue by two independent pathologists, and the samples were staged on the basis of the 8th edition of the Cancer Staging Manual of the American Joint Committee on Cancer. The study was consistent with the ethical guidelines of the Helsinki Declaration and approved by the Ethics Committee.

Cell line and cell culture

Experimental cell lines including A549, PC9, Calu3, H1975 cells were purchased from American Type Culture Collection (ATCC, Manassas, VI). Cells were cultivated in 1640 medium (Corning, NY, USA), supplemented with 1% penicillin/streptomycin (PS; HyClone, Logan, UT, USA) and 10% fetal bovine serum (FBS; PAN-Seratech, Edenbach, Germany), and the incubating temperature was 37 °C, with 5% CO2.

METHOD DETAILS

Immunohistochemistry

The human LUAD tissue microarrays were deparaffinized in xylene and rehydrated through an ethanol series, and antigen was then retrieved in citrate. The cells were treated with 3% hydrogen peroxide for 10 min to inhibit endogenous peroxide activities. Then, the samples were stained using OVOL2 and p62 antibodies at room temperature for 30 min and overnight at 4°C. After washing, tissue microarrays and sections were incubated with secondary antibodies for 1 h at room temperature. The sections were visualised with 3,3-diaminobenzidine solution (ZSGB-Bio) treatment and counterstained with hematoxylin. The percentage immunoreactivity score was classified on a four-point scale: 0. <10% positive cells; 1. 10%–40% positive cells; 2. 40%–70% positive cells; 3. 70%–100% positive cells.

Cell viability assay

Cells were plated in a 96-well plate at 2000cells/well. Then, added 10μL of CCK-8 reagent (Dojindo) in each well and coincubated with the cells in a 37°C incubator for 4h. The OD value of the wavelength at 450nm was measured by an enzyme labeling instrument. The cell proliferation curve was drawn by continuous detection for 3–4 days.

Colony formation assay

For the colony formation assay, 1000 cells in 1640 supplemented with 10% FBS were plated in six-well plates. After 2 weeks of incubation, the surviving colonies were fixed, stained with 0.5% crystal violet, imaged, and counted, and the data are presented as the means ± SDs of triplicate dishes in the same experiment.

Wound healing assay

For the wound healing assay, 1.5-2×10^6 cells were plated in a 6-well plate. The next day, a 10uL pipette tip was used to generate an even wound in the Petri dishes. After the Petri dishes were washed with PBS twice, 2% FBS was added in 1640 medium. The distance of the wound was recorded and calculated by every 3h, and 6 random distances were finally counted. Images were captured with a microscope at 10× magnification. Data processing was performed after 24-48h recording, and GraphPad was used to analyze the distance of two groups on the last time point such as 24h or 48h by paired t-test and mapping the data.

Invasion assay

For the chemotaxis and invasion assay, 24-well plates and 8-μm-pore chemotaxis chambers (Falcon) were used. Especially, for the invasion assay, matrigel was thawed in the ice bath under aseptic conditions, diluted to a concentration of 1 mg/mL with PBS, and frozen at −20°C for further use. Then diluted matrigel was taken out, thawed in the ice bath, plated on the polycarbonate membrane of the 24-well plate transwell chamber with a volume of 50μL, and polymerized into a gel at 37°C for 1h. Then, 20% FBS medium was added to the bottom plate of the 24-well plate (600μL/well), while 200μL of the appropriate concentration of cell suspension was added to the chamber. After the incubating of the well plate containing the chambers was completed, the cells which failed to pass through the chamber were rinsed out. Then the cells were processed with PFA solution, 100% methanol solution, and a three-step staining kit. Three randomly selected fields under the upright microscope were imaged, and the number of cells passing through each field was counted for statistical analysis.

Transfection assay

To obtain lentiviral particles, packaging plasmids (VSVG and ΔR) and expression plasmids (sh-OVOL2, sh-Ctrl, OVOL2, and Vector) were transfected into HEK293T cells using Lipofectamine 2000 (Invitrogen). The lentiviruses were produced by HEK293T cells. PC9 and A549 cells were infected with a lentivirus to produce stable OVOL2 KD and OE cells.

Fluorescence microscopy and confocal microscopy

PC9 and A549 cells were infected with a lentivirus expressing mCherry-GFP-LC3 fusion protein. After the knocking down of OVOL2 or luciferase, samples were examined using an epifluorescent microscope (Olympus BX61, Tokyo, Japan). For confocal microscopy, cells (105) were seeded on a coverslip coated with poly-lysine (Sigma-Aldrich, P6282) in 24-well plates. After being fixed with 4% paraformaldehyde for 15 min at room temperature (RT), the cells were washed 2 times in phosphate-buff-ered saline (PBS, pH 7.4; Invitrogen, 10010023). The coverslips were mounted on glass slides using Vectashield with 4′, 6-dia-midino-2-phenylindole (DAPI; Thermo Scientific, 62248) and examined using a Zeiss LSM510 laser scanning confocal microscope (Carl Zeiss, Jena, Germany).

Transmission electron microscopy

Cells were trypsinized, washed with 0.1M PBS, and fixed with a solution containing 3% glutaraldehyde, and 2% paraformaldehyde (Sigma-Aldrich, 340855 and P6148, respectively) in 0.1 M PBS for 2h at RT. After fixation, the cells were washed with 0.1 M PBS and postfixed with 1% buffered osmium tetroxide (Sigma Aldrich, 75632) for 45 min at RT, and stained with 1% uranyl acetate (Ted Pella, Inc., 19481). After dehydration in graded series ethanol, the cells were embedded in EMbed 812 medium (Electron Microscopy Sciences, 14120) and were polymerized at 70°C for 2d. Ultrathin sections were cut on a Leica Ultra cut microtome (Leica, Vienna, Austria) and stained with uranyl acetate and lead citrate in a Leica EM Stainer. Digital TEM images were acquired from thin sections using a JEM 1010 transmission electron microscope (JEOL, Peabody, MA, USA) at an accelerating voltage of 80 kV equipped with AMT Imaging System (Advanced Microscopy Techniques, Danvers, MA, USA).

QUANTIFICATION AND STATISTICAL ANALYSIS

Clinical data were evaluated using SPSS 26.0 for Windows (SPSS Inc., Chicago, IL).

Student's *t* test was used for comparing two groups, and One-way ANOVA was applied for comparing multiple groups. Spearman correlation coefficient was used to assay the correlation between OVOL2 and P62 expression. Kaplan-Meier analysis was performed to produce overall survival (OS) and disease-free survival (DFS) curves and the log rank test was used to calculate p values. Spearman correlation analysis was used to analyze the relationships between the staining score of OVOL2 and clinicopathological factors. *$p < 0.05$, **$p < 0.01$, ***$p < 0.001$ were considered statistically significant.